

## Effects of channel and potential radiative transitions in the $^{17}\text{O}(\gamma, n_0)^{16}\text{O}$ reaction

R. J. Holt, H. E. Jackson, R. M. Laszewski, J. E. Monahan, and J. R. Specht

Argonne National Laboratory, Argonne, Illinois 60439\*

(Received 26 June 1978)

The angular distribution for the  $^{17}\text{O}(\gamma, n_0)^{16}\text{O}$  reaction was observed throughout the excitation energy region 4.3–7 MeV and at angles of  $90^\circ$  and  $135^\circ$ . The ground-state radiation widths for resonances in this energy region were extracted from the data. The value of the radiation width for the  $d_{5/2} \rightarrow d_{3/2}$  spin-flip transition at 5.08 MeV was found to be approximately 1/3 of the value expected for a pure single-particle transition. The implications that this result has for the nuclear structure of  $^{17}\text{O}$  is discussed. The effects of potential radiative capture were observed directly in a photoneutron reaction for the first time. At the location of the 5.38-MeV,  $3/2^-$  resonance in  $^{17}\text{O}$ , an anomalous symmetric dip was observed in the cross section at both reaction angles. The data were interpreted in terms of a general  $R$ -matrix reaction theory which includes the effects of internal, channel, and potential radiative capture in a self-consistent manner. The neutron channel was defined by incorporating an  $R$ -matrix analysis of the  $^{16}\text{O}(n, n)^{16}\text{O}$  reaction into the present interpretation. The anomalous minimum at 5.38 MeV was found to be due to a unique feature of channel capture. The  $R$ -matrix prediction for the total cross section was extrapolated into the keV region and the significance that this cross section has for stellar nucleosynthesis is discussed.

[NUCLEAR REACTIONS  $^{17}\text{O}(\gamma, n_0)^{16}\text{O}$ ; observed angular distribution;  $E_\gamma = 4.3\text{--}7$  MeV;  $\theta = 90^\circ, 135^\circ$ ;  $R$ -matrix analysis; measured  $\Gamma_{\gamma 0}$  for  $E1$  and  $M1$  resonances.]

### I. INTRODUCTION

The application of general reaction theories to low-energy nuclear reactions involving particles has been extremely successful<sup>1</sup> in recent years. However, reactions involving radiative capture have been more difficult to understand. The difficulties are twofold. First, the inclusion of photon channels in the  $R$ -matrix theory results in a somewhat more complicated formalism<sup>2</sup> for the collision matrix. The long-range nature of the electromagnetic interaction gives rise to a component of the collision matrix which is due to radiative capture in the external region, i.e., beyond the channel radius. These external contributions can be both resonant (channel capture) and direct (potential capture) in nature. Consequently, there are difficulties in distinguishing whether a given resonance arises primarily from channel or internal resonance capture. Secondly, no previous studies of radiative capture have demonstrated unambiguously the effects of channel capture. Many of the radiative capture experiments, especially neutron capture studies,<sup>3</sup> involve a large number of resonances where statistical properties and correlation effects must be invoked in order to describe the nature of the resonances.

In the present work we have chosen to study the interplay among the capture mechanisms in the  $^{17}\text{O}(\gamma, n_0)^{16}\text{O}$  reaction within a few MeV of the neutron threshold. The  $^{17}\text{O}$  nucleus is ideal for this purpose from several points of view. The level

density below 7 MeV is low and individual resonances can be studied in detail. The ground state of  $^{17}\text{O}$  is predominantly single particle in nature, and consequently, the effects of channel and potential capture are expected to be enhanced. Another interesting aspect of this reaction is the observation, for the first time, of the  $M1$  transition probability between the  $d_{5/2}$  ground state and the  $d_{3/2}$  excited state at 5.08 MeV. This transition should represent the ideal example of an  $M1$  single-particle excitation in nuclei. Many theoretical analyses<sup>4</sup> of the  $^{16}\text{O}+n$  system have indicated that the  $d_{3/2}$  resonance is predominantly single particle in nature. Observations of radiative transitions in the oxygen isotopes have proved<sup>5</sup> valuable for determining nuclear structure information. Although numerous shell-model calculations<sup>4,6</sup> have been performed for  $^{17}\text{O}$ , there has been very little experimental information concerning radiative transitions. This has been due to the relative paucity of the  $^{17}\text{O}$  isotope and also to the relatively low neutron threshold.

Therefore, in this work, we report the observation of the differential cross section for the  $^{17}\text{O}(\gamma, n_0)^{16}\text{O}$  reaction throughout the excitation energy region 4.3–7 MeV and at reaction angles of  $90^\circ$  and  $135^\circ$ . The results were interpreted in terms of the theory of radiative capture of Lane and Lynn.<sup>2</sup> The effects of channel and potential capture were observed directly.

In addition, a self-consistent, multilevel  $R$ -matrix analysis was performed of the observations. The results of an  $R$ -matrix analysis<sup>7</sup> of the

$^{16}\text{O}(n,n)^{16}\text{O}$  reaction were incorporated directly into the present formulation in order to ensure that both the  $(n,n)$  and  $(\gamma,n)$  reactions were described simultaneously. The present formalism was found to be more convenient than the traditional treatment of Lane and Lynn.<sup>2</sup> Ground-state radiative widths were extracted from the  $R$ -matrix analysis. The  $R$ -matrix formalism for radiative capture appears in Sec. IV and the results are in Sec. V. The reduced transition probability for the 5.08-MeV  $M1$  excitation was found to be anomalously small. The implications which this anomaly has for nuclear structure and meson exchange effects is discussed in Sec. VI.

Neutron capture reactions are believed<sup>8</sup> to dominate the slow process of stellar evolution. Allen and Macklin<sup>9</sup> have studied the effect which the presence of light elements such as  $^{13}\text{C}$  and  $^{16}\text{O}$  have on the  $s$  process. They concluded that the effects were negligible. In that study the nonresonant  $E1$  direct capture effects were not known and therefore ignored. In the present work, the neutron capture rate for  $^{16}\text{O}$  was estimated using the  $R$ -matrix predictions in the keV region. This estimate indicates that the capture rate is at least an order of magnitude greater than the Allen-Macklin calculation. The discussion of this problem appears in Sec. VII.

## II. EXPERIMENTAL METHOD

The photoneutron spectra were observed with high resolution using the sub-nanosecond time-of-flight spectrometer<sup>10</sup> associated with the Argonne high-current electron accelerator. Electron pulses with a peak current of 200 A, a duration of 35 ps, and an energy of 8.5 MeV were extracted at a rate of 800 Hz from the linac. The electrons were converted to bremsstrahlung photons in a 0.15-cm thick Ag foil. The photons then irradiated the  $^{17}\text{O}$  sample which was in the form of water with an enrichment of 34% in  $^{17}\text{O}$ ; 64.5%  $^{18}\text{O}$ , and 1.5%  $^{16}\text{O}$ . The water sample of dimensions 5 cm  $\times$  6 cm  $\times$  0.5 cm was contained in a thin-walled Al can. The photoneutrons traveled through two well-collimated, 11.5-m flight paths before they were detected in 2.5-cm thick NE110 plastic scintillators. Background effects were determined by replacing the enriched  $\text{H}_2\text{O}$  sample with normal water and repeating the experiment. The raw time-of-flight spectra with background subtracted are shown in Fig. 1. The resonances are shown with the  $\gamma$ -ray energy in MeV. The characteristic features of the data are (i) a nonresonant cross section which rises dramatically with increasing energy, (ii) an asymmetric resonance at 4.55 MeV, (iii) a local minimum in the cross section at 5.38

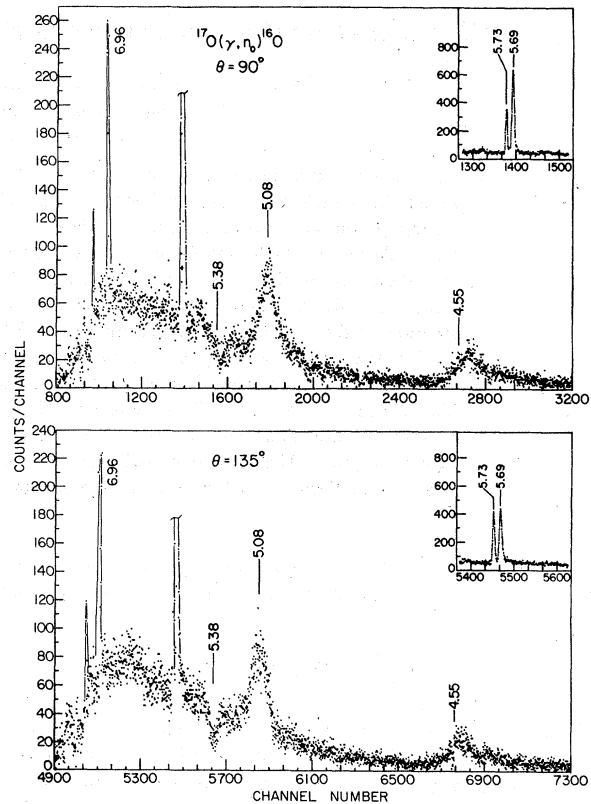


FIG. 1. Observed time-of-flight spectra for the  $^{17}\text{O}(\gamma,n_0)^{16}\text{O}$  reaction at reaction angles of  $90^\circ$  and  $135^\circ$ . The  $\gamma$ -ray energies of the resonances are given in MeV, where  $Q = 4.14$  MeV.

MeV, and (iv) the  $M1$  excitation at 5.08 MeV. The narrow resonances shown in the inset figures demonstrate the high resolution (2.5 keV at  $E_n = 0.5$  MeV and 18 keV at  $E_n = 3$  MeV) of the time-of-flight spectrometer. The magnitudes of the cross sections were determined relative to the well-known cross section for the photodisintegration of the deuteron. The deuterium sample was also in the form of water ( $\text{D}_2\text{O}$ ).

## III. PHOTOEXCITATION PROCESSES OF $^{17}\text{O}$

An  $E1$  transition can excite  $\frac{3}{2}^-$ ,  $\frac{5}{2}^-$ , and  $\frac{7}{2}^-$  resonances in  $^{17}\text{O}$ . These levels emit  $p_{3/2}$ ,  $f_{5/2}$ , and  $f_{7/2}$  neutrons, respectively. An  $M1$  transition excites  $\frac{3}{2}^+$ ,  $\frac{5}{2}^+$ , and  $\frac{7}{2}^+$  states which decay by emitting  $d_{3/2}$ ,  $d_{5/2}$ , and  $g_{7/2}$  neutrons.  $E2$  excitations are  $\frac{1}{2}^+$ ,  $\frac{3}{2}^+$ ,  $\frac{5}{2}^+$ ,  $\frac{7}{2}^+$ , and  $\frac{9}{2}^+$  and can lead to the emission of  $s_{1/2}$ ,  $d_{3/2}$ ,  $d_{5/2}$ ,  $g_{7/2}$ , and  $g_{9/2}$  neutrons. Photon multipolarities of the order of  $M2$  or higher are omitted from the present discussion. We have chosen to ignore  $f$  and  $g$  partial waves for the outgoing neutron, since in this energy range the con-

tribution to neutron potential scattering from these partial waves is negligible.<sup>7,11</sup> Also we have retained only the  $s_{1/2}$  neutron decay for  $E2$  excitations. We found that the inclusion of  $d$ -wave neutron decay into the  $E2$  channel has only a negligible effect. Furthermore, the estimated single-particle  $E2$  ground-state radiation width for the 5.08-MeV,  $\frac{3}{2}^+$  level is only 1% of that expected for an  $M1$  excitation. Figure 2 summarizes the photoexcitations that specifically are included in the present analysis. We note that resonances of  $J^\pi = \frac{1}{2}^-$  can be excited only by an  $M2$  photon, and consequently, the  $p_{1/2}$  neutron channel is not accessible to the photoneutron reaction. For example, the  $\frac{1}{2}^-$  state at an excitation energy of 5.94 MeV is absent from the present spectra. With these approximations the differential cross section<sup>12</sup> can be written

$$\begin{aligned} \frac{d\sigma}{d\Omega} = & \frac{\lambda_\gamma^2}{48} \{4(|U_{p_{3/2}}|^2 + |U_{d_{3/2}}|^2) + 6|U_{d_{5/2}}|^2 + 2|U_{s_{1/2}}|^2 \\ & + [\text{Re}(2.4U_{p_{3/2}}^* U_{d_{3/2}} + 10.998U_{p_{3/2}}^* U_{d_{5/2}} - 5.367U_{p_{3/2}}^* U_{s_{1/2}})]P_1(\cos\theta) \\ & + [-0.4(|U_{p_{3/2}}|^2 + |U_{d_{3/2}}|^2) + 2.743|U_{d_{5/2}}|^2 \\ & + \text{Re}(1.571U_{d_{3/2}}^* U_{d_{5/2}} - (8.198U_{d_{3/2}}^* + 1.789U_{d_{5/2}}^*)U_{s_{1/2}})]P_2(\cos\theta)\}, \end{aligned} \quad (1)$$

where the amplitudes  $U_{lJ}$  are the collision matrix elements for the photoneutron reaction. The manner in which the collision matrix is related to the  $R$ -matrix theory is given in the following section.

#### IV. R-MATRIX ANALYSIS

Following the example of Lane and Thomas,<sup>13</sup> we treat the photoreaction within the framework of first order perturbation theory assuming that (i) the electromagnetic part of the interaction is small in comparison to the hadronic interaction, (ii) only one photon, either real or virtual, exists at any one time in each photoreaction process. The first assumption is reasonable for the present example since the photoneutron cross sections are a factor of  $10^3$  to  $10^4$  smaller than the neutron scattering cross sections. Our theoretical approach to this problem will be very similar to the Lane and Lynn theory,<sup>2</sup> initially. However, upon application of the theory of radiative capture to the  $^{17}\text{O}(\gamma, n_0)^{16}\text{O}$  reaction we treat the external capture portion in a different manner.

The collision matrix will be expressed in terms of that part of the Hamiltonian  $H^{(\mathcal{L})}$  which electromagnetically couples the photon to the nucleons. In order to calculate that matrix element it is necessary to introduce the wave function  $\psi_{E(J)}$  which describes the neutron-nucleus state and a

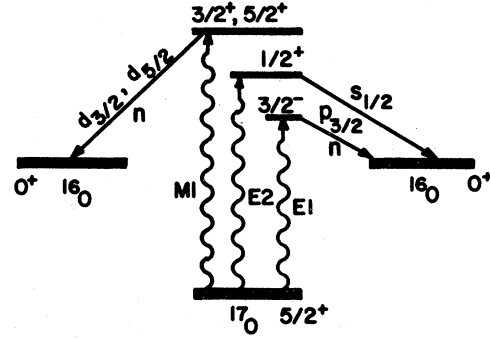


FIG. 2. Photoexcitation processes of  $^{17}\text{O}$ . Only those excitation and neutron decay processes that were invoked in the present  $R$ -matrix analysis are illustrated.

final wave function  $\psi_{f(J_f)}$  which describes the nucleus with all nucleons in its ground state. The collision matrix is

$$\begin{aligned} U_{\gamma E_f, c}^{(J)} = & \left[ \frac{8\pi(\mathcal{L}+1)}{\mathcal{L}\hbar} \right]^{1/2} \frac{k_\gamma^{\mathcal{L}+1/2}}{(2\mathcal{L}+1)!!} \\ & \times \frac{\langle \psi_{f(J_f)} || H^{(\mathcal{L})} || \psi_{E(J)} \rangle}{(2J+1)^{1/2}}, \end{aligned} \quad (2)$$

where  $k_\gamma = E_\gamma/\hbar c$  is the photon wave number and the subscript  $c$  refers to the final particle channel with the quantum numbers ( $sJ$ ). Here  $s$  is the channel spin,  $l$  is the orbital angular momentum,  $\vec{J} = \vec{l} + \vec{s}$  is the total angular momentum, and  $\mathcal{L}$  is the multipolarity. The radial integration implied by Eq. (2) must be performed in two parts: from the origin to the channel radius and from the channel radius to infinity. Inside the channel radius  $R$  the wave function  $\psi_{E(J)}$  can be expanded in terms of a complete set of states  $X_\lambda$

$$\Psi_{E(J)} = i\hbar^{1/2} e^{-i\phi_c} \sum_{\lambda\mu} A_{\lambda\mu} \Gamma_{\mu c}^{1/2} X_{\lambda(J)}, \quad r \leq R \quad (3)$$

where  $\phi_c$  is the hard-sphere phase shift,  $\Gamma_{\mu c}$  is the width of the level  $\mu$  in channel  $c$ . Equation (3) corresponds to unit incoming flux in channel  $c$ .  $A_{\lambda\mu}$  is the matrix transformation which relates the internal wave function and the observed reso-

nances.

$$(A^{-1})_{\lambda\mu} = (E_\lambda - E)\delta_{\lambda\mu} - \xi_{\lambda\mu},$$

where  $E_\lambda$  is a level energy,  $\delta_{\lambda\mu}$  is the Kronecker  $\delta$  function, and  $\xi$  is written in terms of the shift factor  $S_c$ , the boundary condition constant  $b_c$ , and the penetration factor  $P_c$  as

$$\xi_{\lambda\mu} = \sum_c [(S_c - b_c) + iP_c] \gamma_{\lambda c} \gamma_{\mu c},$$

where the  $\gamma_{\lambda c}$  are the reduced width amplitudes. In the exterior region the wave function  $\psi_{E(J)}$  can be written in the customary manner in terms of the incoming  $I_c$  and outgoing  $O_c$  spherical waves

$$\Psi_{E(JM)} = v_c^{1/2} [I_c(k_c r) - U_{cc}^{(J)} O_c(k_c r)] \varphi_{c(JM)}, \quad r \geq R \quad (4)$$

where we have assumed that  $c$  is the only open particle channel and have neglected contributions from closed channels. Here,  $v_c$  is the particle

speed,  $\varphi_{c(JM)} = r^{-1}(i^l Y_{lM})\psi_c$  is the surface function.  $U_{cc}$  is the collision function for elastic scattering in channel  $c$ . For the moment we write the collision function in the form

$$U_{cc}^{(J)} = e^{-2i\phi_c} \left( 1 + i \sum_{\lambda\mu} A_{\lambda\mu} \Gamma_{\mu c}^{1/2} \Gamma_{\lambda c}^{1/2} \right). \quad (5)$$

The last expression implies that we include all possible resonances in the analysis, i.e., there is no explicit provision for the effects of distant levels on the energy interval of interest. For the final interpretation of the experimental results, the level representation Eq. (5) will be replaced with an expression for  $U_{cc}^{(J)}$  in terms of a channel representation. However, it is more instructive for the present argument to consider the more traditional form of  $U_{cc}^{(J)}$  as given by Eq. (5). Substitute Eq. (5) into Eq. (4) and then Eqs. (3) and (4) into Eq. (2); the integration naturally splits into an internal segment ( $r \leq R$ ) and an external region ( $r > R$ ). The collision matrix becomes

$$U_{\gamma_{\mathcal{L}f},c}^{(J)} = ie^{-i\phi_c} \sum_{\lambda\mu} A_{\lambda\mu} \Gamma_{\lambda c}^{1/2} \Gamma_{\mu f}^{1/2} + \left[ \frac{8\pi(\mathcal{L}+1)}{\mathcal{L}\hbar v_c} \right]^{1/2} \frac{k_\gamma^{\mathcal{L}+1/2}}{(2\mathcal{L}+1)!!} (2J+1)^{-1/2} \langle \Psi_{f(J_f)} \| H^{(\mathcal{L})} \| (I_c - e^{-2i\phi_c} O_c) \varphi_{c(J)} \rangle \\ - \left[ \frac{8\pi(\mathcal{L}+1)}{\mathcal{L}\hbar v_c} \right]^{1/2} \frac{k_\gamma^{\mathcal{L}+1/2}}{(2\mathcal{L}+1)!!} (2J+1)^{-1/2} i e^{-2i\phi_c} \sum_{\lambda\mu} A_{\lambda\mu} \Gamma_{\lambda c}^{1/2} \Gamma_{\mu c}^{1/2} \langle \Psi_{f(J_f)} \| H^{(\mathcal{L})} \| O_c \varphi_{c(J)} \rangle, \quad (6)$$

where we have made the identification that

$$\Gamma_{\gamma_{\mathcal{L}f}}^{1/2} = \left[ \frac{8\pi(\mathcal{L}+1)}{\mathcal{L}} \right]^{1/2} \frac{k_\gamma^{\mathcal{L}+1/2}}{(2\mathcal{L}+1)!!} \frac{\langle \Psi_{f(J_f)} \| H^{(\mathcal{L})} \| X_{\lambda(J)} \rangle}{(2J+1)^{1/2}}.$$

This  $\gamma$ -ray width is that portion of the radiative capture strength that is due to the matrix element in the interior region. We note that this width has a real value. This width is sometimes referred to as the compound nuclear part of the radiative capture. It is expected that these radiative widths, in general, will not be correlated with the particle widths as in the case of direct capture resonances. Nevertheless, the first term in Eq. (6) is a resonant component. The second term contains no pole terms, and therefore, gives rise to a nonresonant component. This term is referred to as hard-sphere capture, since it depends only on the hard-sphere phase shift. The final term is due to resonant capture which occurs in the external region, i.e., outside the channel radius. This process is referred to as channel capture. The contribution from the last two terms in Eq. (6) is due to the long-range nature of the electromagnetic interaction. The reduced radiative width for the channel capture component can be identified as

$$(\delta\Gamma_{\mu f,c})^{1/2} = \left[ \frac{8\pi(\mathcal{L}+1)}{\mathcal{L}\hbar v_c} \right]^{1/2} \frac{k_\gamma^{\mathcal{L}+1/2}}{(2\mathcal{L}+1)!!} e^{-i\phi_c} (2J+1)^{-1/2} \Gamma_{\mu c}^{1/2} \langle \Psi_{f(J_f)} \| H^{(\mathcal{L})} \| O_c \varphi_{c(J)} \rangle. \quad (7)$$

Then the form for the collision matrix becomes

$$U_{\gamma_{\mathcal{L}f},c}^{(J)} = ie^{-i\phi_c} \sum_{\lambda\mu} A_{\lambda\mu} \Gamma_{\lambda c}^{1/2} [\Gamma_{\mu \gamma f}^{1/2} - (\delta\Gamma_{\mu \gamma f})^{1/2}] + U_{\gamma_{\mathcal{L}f},c}^J(\text{H. S.}), \quad (8)$$

where  $U_{\gamma_{\mathcal{L}f},c}^J(\text{H. S.})$  is the hard-sphere component. Here the  $(\delta\Gamma_{\mu \gamma f})^{1/2}$  is in general a complex quantity, since the outgoing wave function  $O$  is complex. It will be shown that the complex nature of  $(\delta\Gamma_{\mu \gamma f})^{1/2}$  gives rise to unique features of radiative

capture spectra. The observed radiative width  $\Gamma_{\gamma_0}$  is given by  $\Gamma_{\gamma_0} = |\Gamma_{\mu \gamma f}^{1/2} - (\delta\Gamma_{\mu \gamma f})^{1/2}|^2$ .

Although the foregoing arguments are general with regard to the particle channel  $c$ , we now specialize to the neutron channel. Most radiative

capture experiments involve slow neutrons (<100 keV) so that  $O_i = F_i + iG_i$  essentially becomes a real quantity. In that case, resonances with radiative width amplitudes of  $\Gamma_{\mu, \gamma f}^{1/2}$  or  $(\delta\Gamma_{\mu, \gamma f})^{1/2}$  become indistinguishable in their energy dependence. However, in the present case the imaginary part of  $(\delta\Gamma_{\mu, \gamma f})^{1/2}$  can become comparable in magnitude with the real part in the MeV region for  $p$ -wave neutron capture. (See Fig. 3.) A good example of this is the 5.38-MeV resonance in  $^{17}\text{O}$ . The interference of the resonant amplitude with the nonresonant background term produces a nearly symmetric minimum in the observed cross section. Figure 4 shows the deduced differential cross section as a function of energy along with the results of an  $R$ -matrix analysis. We based this analysis upon Eq. (6) and ignored consistency with the neutron elastic scattering observations for the moment. The wave function for the final state  $^{17}\text{O}$  was taken to be a Whittaker function

$$\Psi_{f_i J_f} = (2/R)^{1/2} \theta_{fc_f} \frac{W_{c_f}(k_f r)}{W_{c_f}(k_f R)} \varphi_{c_f}(J_f, M_f), \quad (9)$$

where  $\theta_{fc_f}$  is the dimensionless reduced width of Lane and Thomas

$$\theta_{fc_f} = \gamma_{fc_f} / (\hbar^2 / MR^2)^{1/2}$$

and  $k_f$  is the wave number corresponding to the binding energy of the neutron in  $^{17}\text{O}$ . The Whittaker function for electrically neutral particles is given by

$$W(k, r) = \frac{e^{-kfr}}{\Gamma(1)} \int_0^\infty t^1 e^{-t} (1 + t/2kfr)^1 dt. \quad (10)$$

The parameters which were adjusted in order to obtain the fitted curve in Fig. 4 are  $\theta_{if J_f}$  and the  $\Gamma_{\mu, \gamma f}$ 's. The neutron widths were held fixed at the experimentally determined values. The para-

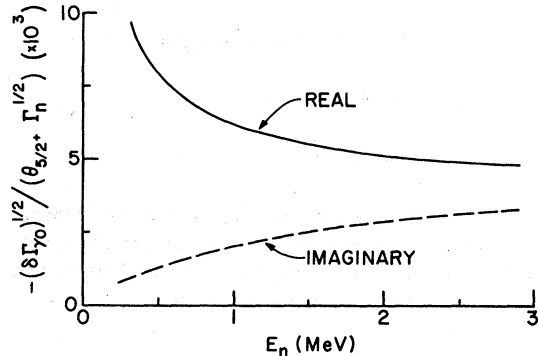


FIG. 3. Real and imaginary components of the  $E1$  radiative channel capture for  $p_{3/2}$  neutrons. In the MeV region the imaginary part is not negligible in comparison with the real component.

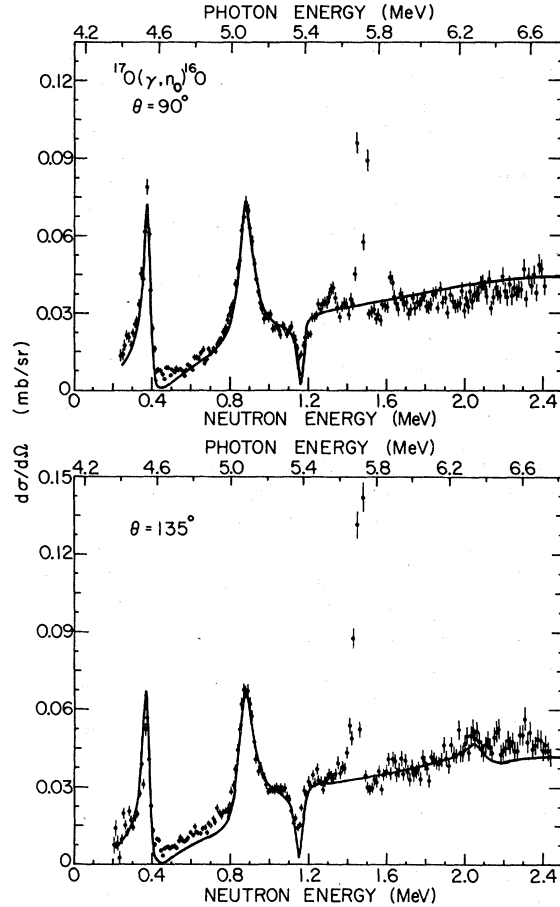


FIG. 4.  $R$ -matrix interpretation of the differential cross section for the  $^{17}\text{O}(\gamma, n_0)^{16}\text{O}$  reaction. The points represent the observations while the curves represent the results of a "hard-sphere" external capture model.

eters for this analysis are given in Table I.

This simple procedure ignores the effects of distant levels in the neutron channel. These effects should enter the collision matrix in expression (5). Despite this simplification, the essential features of the  $^{17}\text{O}(\gamma, n_0)^{16}\text{O}$  data can be explained. Since distant levels in the neutron elastic channel are omitted, the smoothly varying nonresonant capture is dominated by hard-sphere capture of an  $E1$  photon and the emission of a  $p_{3/2}$  neutron. In fact, an attempt to include  $M1$  "hard-sphere" capture in this simple model worsened the agreement of the theory with the experiment. This is not surprising since a simple hard-sphere model will not explain nonresonant neutron scattering from  $^{16}\text{O}$ . The asymmetry of the 4.55-MeV,  $\frac{3}{2}$  resonance is also explained by this model. The observed asymmetry is due to the interference of the nonresonant amplitude, the last term in Eq. (8), with the resonant amplitude.

TABLE I.  $R$ -matrix parameters for the hard-sphere external radiative capture model. Note that channel capture is included explicitly only in the  $p_{3/2}$  neutron channel,  $\theta_{5/2^+} = -1.08$ ,  $R_c = 4.93$  fm.

$M\mathcal{L}$	$J^\pi$	$E_\gamma$ (MeV)	$\Gamma_n$ (MeV)	$\Gamma_{\gamma f}^{1/2}$ (eV) <sup>1/2</sup>
E1	$\frac{3^-}{2}$	4.549	0.043	1.41
		5.378	0.038	1.37
		7.532	0.442	3.31
M1	$\frac{3^+}{2}$	5.077	0.094	-0.99
E2	$\frac{1^+}{2}$	6.354	0.130	-0.25

From Fig. 4, we find that the channel capture width has a predominately real value near  $E_n = 440$  keV. Thus the 4.55-MeV resonance has a widely observed asymmetric shape.<sup>14</sup> On the other hand, the 5.38-MeV resonance has a symmetric interference pattern. This effect can arise only from the interference of a resonant term, which has a nearly pure imaginary radiative width, with the nonresonant amplitude. Again from Fig. 3 we see that the imaginary component of the channel capture amplitude for a 1.3-MeV neutron is somewhat more comparable with the real part. The conditions for a symmetric interference minimum are met if we allow the radiative width of the internal capture component  $\Gamma_{\mu\gamma f}^{1/2}$  of Eq. (8) to offset the real part of the channel capture term  $(\delta\Gamma_{\mu\gamma f})^{1/2}$ . Indeed, these conditions give the best representation of the observations as shown in Fig. 4. In this way, the channel capture effects enter in a unique way.

These interference effects can be demonstrated in a simple manner by considering a single level and a direct component  $D$  with the same spin and parity as that of the level. The collision matrix becomes

$$U_{\gamma n} = ie^{-i\phi_i} \left[ \frac{\Gamma_n^{1/2} [\Gamma_{\gamma f}^{1/2} - (\delta\Gamma_{\gamma f})^{1/2}] + D}{E_\gamma - E - i\Gamma/2} \right].$$

The total  $(\gamma, n)$  cross section for this example becomes

$$\sigma_{\gamma n} = \pi g_J \lambda_\gamma^2 \left\{ \frac{4[\Gamma_{\gamma 0}\Gamma_n + D\Gamma_n^{1/2}\text{Im}(\delta\Gamma_{\gamma f})^{1/2}]}{\Gamma^2(1+X^2)} + \frac{4D\Gamma_n^{1/2}X[\Gamma_{\gamma f}^{1/2} - \text{Re}(\delta\Gamma_{\gamma f})^{1/2}]}{\Gamma(1+X^2)} + D^2 \right\},$$

$$U_{\gamma n}^{(iJ\mathcal{L})} = ie^{-i\phi_i} \sum_{\lambda\mu} A_{\lambda\mu} \Gamma_{\lambda i J}^{1/2} \Gamma_{\mu \gamma f i J}^{1/2} + \left( \frac{8\pi(\mathcal{L}+1)^{1/2}}{\mathcal{L}\hbar\gamma_n} \right)^{1/2} \frac{k_\gamma^{\mathcal{L}+1/2}}{(2\mathcal{L}+1)!!} (2J+1)^{-1/2} \langle \Psi_{\lambda J_f} || H^{(\mathcal{L})} || (I_i - e^{2i\delta_{iJ}} Q_i) \varphi_{iJ} \rangle. \quad (12)$$

where  $\Gamma_{\gamma 0} \equiv |\Gamma_{\gamma f}^{1/2} - (\delta\Gamma_{\gamma f})^{1/2}|^2$  is the ground-state radiation width and  $X \equiv (2/\Gamma)(E_\gamma - E)$ . Clearly, the first term in the above expression gives rise to symmetric resonance shapes, while the second term is asymmetric about  $X=0$ . It is also evident that if  $|\text{Im}(\delta\Gamma_{\gamma f})^{1/2}| \ll |\text{Re}(\delta\Gamma_{\gamma f})^{1/2}|$ , then  $\Gamma_{\gamma f}^{1/2}$  and  $(\delta\Gamma_{\gamma f})^{1/2}$  become indistinguishable. However, if  $\Gamma_{\gamma f}^{1/2} = \text{Re}(\delta\Gamma_{\gamma f})^{1/2}$ , then a novel resonance pattern is possible in the photoneutron spectrum

$$\sigma_{\gamma n} = \pi g_J \lambda_\gamma^2 \frac{4[\Gamma_{\gamma 0}\Gamma_n + D\Gamma_n^{1/2}\text{Im}(\delta\Gamma_{\gamma f})^{1/2}] + D^2}{\Gamma^2(1+X^2)}.$$

With these conditions the resonance shape becomes symmetric and can give rise to constructive or destructive interference with the direct component. In the case of the 5.38-MeV,  $\frac{3^-}{2}$  resonance,  $[\Gamma_{\gamma 0}\Gamma_n + D\Gamma_n^{1/2}\text{Im}(\delta\Gamma_{\gamma f})^{1/2}] < 0$ , and consequently, a symmetric minimum results in the cross section. This "window" in the  $(\gamma, n)$  cross section is a unique feature of radiative channel capture interfering with potential capture.

In order to obtain a self-consistent interpretation of the  $^{16}\text{O}+n$  system, it would be necessary to introduce the effects due to distant resonances into expression (5). However, in the energy region of interest only two channels are open: photon and neutron. Thus, it is convenient to replace Eq. (5) by

$$U_{cc}^{(iJ)} = e^{2i\delta_{iJ}}, \quad (11)$$

where  $\delta_{iJ}$  are the scattering phase shifts. Now these phase shifts are already known from neutron elastic scattering measurements. Hickey *et al.*<sup>7</sup> has obtained these phase shifts in terms of  $R$ -function parameters. These  $R$ -function parameters describe the observed total cross section, angular distributions, and polarizations in the neutron energy region 0-4 MeV. The phase shifts are computed from

$$\delta_{iJ} = -\phi_i + \tan^{-1} \{ R_{iJ} P_i / [1 - R_{iJ}(S - b_{iJ})] \},$$

where  $R_{iJ}$  is the  $R$  function

$$R_{iJ} = \sum_{\lambda} \frac{\gamma_{\lambda i J}^2}{E_{\lambda i J} - E} + R_0.$$

Here  $R_0$  is the contribution due to distant levels and  $\gamma_{\lambda}^2$  is the reduced width. By substituting expression (11) into (4), the collision matrix for the photoneutron process simplifies to

As one can see from the last expression, it is no longer easy to separate hard-sphere capture from channel capture. The two external radiative capture effects merge into a single term.

### V. RESULTS AND DISCUSSION

The  $R$ -function parameters used to evaluate  $\delta_{lJ}$  are given in Table II. These parameters were taken from Ref. 7 and the width of the  $E_n = 1.3$ -MeV resonance ( $\frac{3}{2}^-$ ) was increased by 10% in order to give better agreement with the present data. The results of this analysis are compared with the observations in Fig. 5. One major improvement in this interpretation is that the minimum at 5.38 MeV is not as deep as in the "hard-sphere" analysis. The main reason for this is that this minimum is filled in from capture involving tails of distant levels in the neutron channel. From Table II we see that the  $p_{3/2}$  channel has a large contribution ( $R_0 = 0.54$ ) from distant levels. This strongly affects the  $E1$  nonresonant capture. This can be seen by comparing the deduced values of  $\theta_{l_f J_f}$  for the hard-sphere capture predictions and the self-consistent analysis. The value of this reduced width determines the size of the direct capture component. In the hard-sphere case  $\theta_{5/2^+}^2 = 1.17$  and in the self-consistent model  $\theta_{5/2^+}^2 = 0.35$ . This indicates that the effects of distant levels in the neutron channel can contribute a sizeable fraction to the direct capture process. The final parameters which describe the photo-neutron reaction in  $^{17}\text{O}$  are given in Table III. One should not take the values of  $\Gamma_{uyf}$  too seriously for the resonances at  $E_\gamma = 7.21$  and 7.53 MeV since the radiative widths assigned to these levels also include the effects of distant resonances.

The above analysis is reminiscent of the Christy and Duck,<sup>15</sup> Tombrello and Parker,<sup>16</sup> and more

TABLE II.  $R$ -matrix parameters which were used in the present analysis for the  $^{16}\text{O}(n, n)^{16}\text{O}$  reaction. [Note that the  $p_{1/2}$  parameters are not necessary for the  $(\gamma, n)$  channel.]

$l_J$	$E_{lJ}$ (MeV)	$\gamma_{lJ}^2$ (MeV)	$R_{0lJ}$	$b_{lJ}$
$s_{1/2}$	-3.272	0.46	0	0
	2.35	0.056		
$p_{3/2}$	0.392	0.165	0.54	-0.405
	1.305	0.033		
	3.445	0.214		
$d_{3/2}$	0.69	0.816	0.06	-1.194
	1.834	0.014		
	3.300	0.187		
	4.160	0.012		
$d_{5/2}$	-4.143	0.80	0	-0.787

TABLE III.  $R$ -matrix parameters for the  $^{17}\text{O}(\gamma, n_0)^{16}\text{O}$  reaction for  $\theta_{5/2^+} = -0.59$ ,  $R_c = 4.93$  fm.

$M\mathcal{L}$	$J^\pi$	$E_\gamma$ (MeV)	$\Gamma_n$ (MeV)	$\Gamma_{\gamma f}^{1/2}$ (eV) <sup>1/2</sup>
$E1$	$\frac{3}{2}^-$	4.549	0.043	0.49
		5.378	0.038	0.65
		7.532	0.442	0.71
$M1$	$\frac{3}{2}^+$	5.077	0.094	-0.69
		7.213	0.255	1.44
$E2$	$\frac{1}{2}^+$	6.354	0.130	-0.22

recently, Rolfs<sup>17</sup> extranuclear capture model. Their formulation was applied to low-energy charged-particle radiative capture. In the sense that they employed known phase shifts, which describe the elastic channel, in order to compute capture in the external region there is some similarity. However, the present work is the first

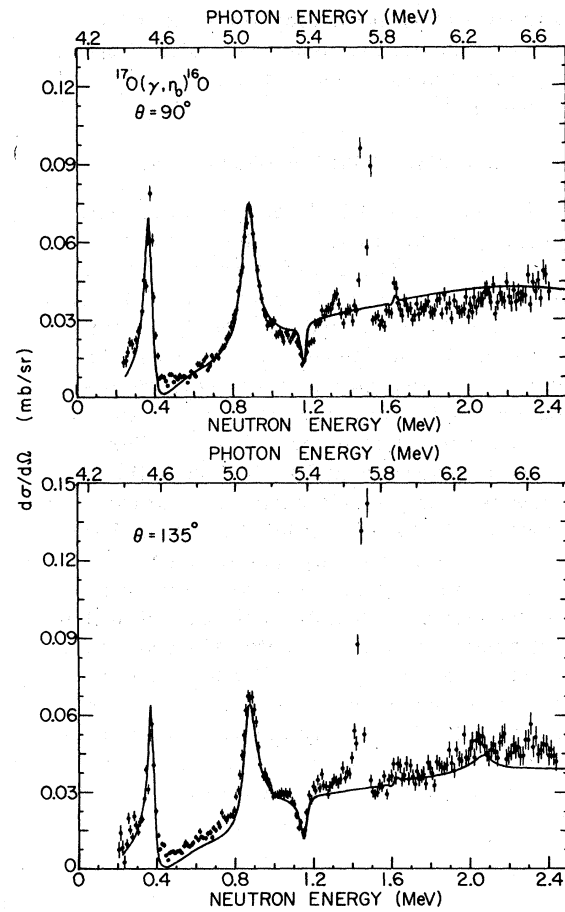


FIG. 5. Final  $R$ -matrix analysis of the observations of the  $^{17}\text{O}(\gamma, n_0)^{16}\text{O}$  reaction. The parameters used in this analysis, Tables III and IV, also describe the  $^{16}\text{O}(n, n)^{16}\text{O}$  reaction. The interference minimum at 5.38 MeV is not as deep as that given by the simple hard-sphere model.

description of a capture process which treats both internal and external capture in a self-consistent manner and completely within the framework of a general multi-level  $R$ -matrix formulation. In particular, Domingo<sup>18</sup> applied the extranuclear capture model to the study of  $^{16}\text{O}(p, \gamma)^{17}\text{F}$  reaction. Since  $^{17}\text{F}$  is the mirror nucleus of  $^{17}\text{O}$ , one might expect the properties of the two nuclei to be similar. For example, we know that the spectroscopic factors for the ground states are approximately unity from studies<sup>19, 20</sup> of the  $^{16}\text{O}(d, n)^{17}\text{F}$  and  $^{16}\text{O}(d, p)^{17}\text{O}$  reactions. Similarly, Domingo found that the Lane reduced width  $\theta_{5/2}^2(^{17}\text{F}) = 0.38$ ; whereas, we obtain  $\theta_{5/2}^2(^{17}\text{O}) = 0.35$ . This remarkably good agreement indicates that direct radiative capture reactions can play an important part in nuclear spectroscopy.

The ground-state radiation width for the 4.55-MeV,  $\frac{3}{2}^-$  resonance was found to be 0.4 eV. The weak-coupling model of Engeland and Ellis<sup>5</sup> predict this  $E1$  excitation to be 1.9 eV. This discrepancy is not overly surprising since the model also fails to explain the observed<sup>21</sup> ratio of spectroscopic factors for 4.55- and 5.38-MeV,  $\frac{3}{2}^-$  resonances in  $^{17}\text{O}$ .

## VI. MAGNETIC DIPOLE EXCITATIONS

The  $M1$  resonance at 5.08 MeV results from the  $d_{5/2} \rightarrow d_{3/2}$  spin-flip transition. To first order the  $\frac{5}{2}^+$  ground state of  $^{17}\text{O}$  can be thought of as a  $d_{5/2}$  neutron in orbit about an  $^{16}\text{O}$  core. The  $^{16}\text{O}$  nucleus is believed<sup>6</sup> to be described, primarily, in terms of  $0p$ - $0h$ ,  $2p$ - $2h$ , and  $4p$ - $4h$  configurations. This model of the  $^{17}\text{O}$  ground state is reasonable since the spectroscopic factor for the ground state was determined<sup>19</sup> to be approximately unity. Furthermore, the  $\frac{3}{2}^+$  resonance at 5.08 MeV is believed<sup>5</sup> to be predominantly single particle in nature. The spectroscopic factor of this level has been determined<sup>11</sup> from neutron elastic scattering to be  $\sim 0.7$ . In addition, the magnetic dipole moment for the  $^{17}\text{O}$  nucleus is within a few percent of the Schmidt single-particle estimate. Consequently, we expect, *a priori*, that the  $M1$  excitation at 5.08 MeV to be near the single-particle estimate. The single-particle value can be obtained readily from the following argument. The reduced transition probability between two spin-orbit partners is given by

$$B(M1; l - \frac{1}{2} \rightarrow l + \frac{1}{2}) = \left( \frac{l+1}{l} \right) |\langle \Psi^{(l+1/2)} || M1 || \Psi^{(l-1/2)} \rangle|^2. \quad (13)$$

If we consider the bare  $M1$  operator for a single neutron transition, then the reduced transition probability becomes

$$B_\nu(M1; l - \frac{1}{2} \rightarrow l + \frac{1}{2}) = \frac{3(l+1)}{(2l+1)\pi} \mu_n^2 \left( \frac{e\hbar}{2M_p c} \right)^2 \left| \int_0^\infty u_{l-1/2} u_{l+1/2} dr \right|^2,$$

where  $\mu_n$  is the magnetic moment in nuclear magnetons of the neutron. The value of the radial overlap integral was taken to be unity for the present argument. This is a reasonable approximation since there is no change in the orbital angular momentum between the initial and final states. For the  $d_{3/2} \rightarrow d_{5/2}$  spin-flip transition we have

$$B_\nu(M1; \frac{3}{2}^+ \rightarrow \frac{5}{2}^+) = 2.09 \left( \frac{e\hbar}{2M_p c} \right)^2,$$

and the ground-state radiation width for the 5.08-MeV resonance is

$$\Gamma_{\gamma 0, \nu}^{(s.p.)} = 3.17 \text{ eV}.$$

From Table IV we see that the observed  $\Gamma_{\gamma 0}$  is 1.0 eV, less than a third of the single-particle estimate. This observed extinction of  $M1$  strength indicates that nuclear structure effects or meson exchange corrections have an important effect on the magnetic dipole transition.

One expects that the dynamic properties of nuclei to be more sensitive to the details of nuclear structure and meson exchange than the static properties. For example, the magnetic dipole transition matrix element is squared in Eq. (13), but the static magnetic dipole moment only involves the expectation value of the spin operator.

Konopka, Gari, and Zabolitzky<sup>22</sup> have estimated that meson currents increase the magnitude of the magnetic dipole moment of  $^{17}\text{O}$  by  $\sim 15\%$ . Thus, the effect on the 5.08-MeV spin-flip transition should be  $\lesssim 30\%$ . The quadratic nature of the reduced transition probability can also give rise to marked sensitivity to the particle-hole structure of the  $^{17}\text{O}$  ground state and the 5.08-MeV resonance. The  $M1$  operator can connect not only

TABLE IV. Deduced ground-state radiation widths for levels in  $^{17}\text{O}$ .

$M\mathcal{L}$	$J^\pi$	$E_\gamma$ (MeV)	$\Gamma_{\gamma 0}$ (eV)	$g_J \Gamma_{\gamma 0} \Gamma_n / \Gamma$ (eV)
E1	$\frac{3}{2}^-$	4.549	0.42	0.14
	$\frac{1}{2}^-$	5.378	0.06	0.02
M1	$\frac{7}{2}^+$	5.690	0.4 <sup>a</sup>	0.27 <sup>a</sup>
	$\frac{3}{2}^+$	5.077	1.0	0.33
E2	$\frac{1}{2}^+$	6.354	<0.07	<0.012
E1, M1	$\frac{3}{2}^-, \frac{5}{2}^-, \frac{7}{2}^+$	5.729		1.5 <sup>a</sup>

<sup>a</sup> Value was deduced from area analysis.

1p-0h states but also 3p-2h and 5p-4h states in  $^{17}\text{O}$ . In order to arrive at a large reduction in the  $M1$  transition probability, the 3p-2h or 5p-4h matrix elements must be opposite in sign to the 1p-0h part. More precisely, this result indicates either that the 3p-2h or 5p-4h components of the wave function of the  $\frac{3}{2}^+$  resonance are opposite in sign to those of the ground state or that the 1p-0h part of the  $\frac{3}{2}^+$  level is opposite in sign to that of the ground state.

The nuclear coexistence model<sup>23</sup> potentially provides another solution to this problem. In this model one can think of the ground state and the 5.08-MeV resonance of  $^{17}\text{O}$  as possessing a spherical component plus a neutron (single-particle) and a deformed part (collective). The  $M1$  operator can then connect the single-particle component of the ground state to that of the  $\frac{3}{2}^+$  level, and likewise, the collective part to that of the  $\frac{3}{2}^+$  level. Thus, a reduction of the  $M1$  strength can be realized if the deformed part of the 5.08-MeV,  $\frac{3}{2}^+$  level is opposite in sign to the collective component of the ground state. Clearly, a detailed calculation which includes the structure of the  $\frac{3}{2}^+$  resonance is necessary in order to account for the present anomaly.

## VII. ASTROPHYSICAL IMPLICATIONS

Neutron capture studies have contributed greatly to our understanding of the slow process in nucleosynthesis. The  $s$  process is believed to be significant in the formation of heavy nuclei with atomic mass greater than that of the  $^{56}\text{Fe}$  nucleus. Macklin and Gibbons<sup>9</sup> have tabulated the neutron capture reaction rates for a variety of nuclei and for various stellar temperatures. The reaction rate is the total neutron capture cross section times the neutron speed weighted by a Maxwell-Boltzmann distribution of neutron speeds in the stellar medium of temperature  $T$ . The reaction rate is given by

$$\langle \sigma_m(v)v \rangle = \frac{4}{\pi^{1/2}} \int_0^\infty \sigma_m(v) (v/v_T)^3 e^{-(v/v_T)^2} dv, \quad (14)$$

where  $v_T = (2kT/\mu)^{1/2}$ ,  $k$  is the Boltzmann constant, and  $\mu$  is the reduced mass of the neutron-nucleus system. Macklin and Gibbons have derived a simpler expression for the above equation by assuming that the capture cross section is due almost entirely to the high-energy tail  $s$ -wave thermal capture and to narrow resonances. In fact, it was assumed in Ref.

8 that a resonance could be represented by a Dirac  $\delta$  function in energy. Thus, the integration implied by Eq. (14) could be performed very simply. One must note that the Macklin-Gibbons

formula, then, applies only to narrow resonances. Unfortunately, this assumption was ignored in the work of Allen and Macklin.<sup>9</sup> In that study the Macklin-Gibbons formula was applied to fast neutron capture data for  $^{16}\text{O}$ . Two main features were therefore overlooked: (1) the low-energy tail of the broad 44-keV wide,  $\frac{3}{2}^-$  level at  $E_{\text{ex}} = 4.55$  MeV and (2) direct nonresonant  $E1$  capture which extends into the keV region. Allen and Macklin wished to determine the extent to which neutron capture in  $^{16}\text{O}$  competes with the  $^{56}\text{Fe}$  capture rate, and consequently, whether or not  $^{16}\text{O}$  mitigates the  $s$  process. We have reevaluated the cross section  $\langle \sigma \rangle_{kT} = \langle \sigma_m(v)v \rangle / v_T$  by performing the integral in Eq. (14) numerically using a single-level formula for  $\sigma_m(v)$ . The resonance parameters used were those given in Ref. 9 and the characteristic stellar temperature was chosen so that  $kT = 30$  keV. The contribution  $\langle \sigma \rangle_{kT}$  from the 4.55-MeV resonance alone was calculated to be a factor of 120 times greater than the value determined from the Macklin-Gibbons formula. This leads to a corrected value of  $\langle \sigma \rangle_{kT=30} = 4.9 \mu\text{b}$  quoted in Ref. 9 for  $^{16}\text{O}$ .

This estimate does not include the effects of nonresonant direct capture. A lower limit of the Maxwell-Boltzmann weighted capture cross section for  $kT = 30$  keV can be obtained from the present  $R$ -matrix analysis, using the parameters of Table III, the  $R$ -matrix prediction for the total cross section for the  $^{17}\text{O}(\gamma, n_0)^{16}\text{O}$  reaction is shown in Fig. 6 throughout the energy range 4.14–7 MeV. It is clear from this figure that the low-energy tail of the 4.55-MeV resonance cannot be neglected in this kind of analysis.

The total predicted capture cross section for ground-state radiation was determined by detailed balance and used to obtain  $\langle \sigma \rangle_{0, kT=30} = 2.2 \mu\text{b}$  from Eq. (14). This value is a lower limit since only ground-state transitions are considered. However,

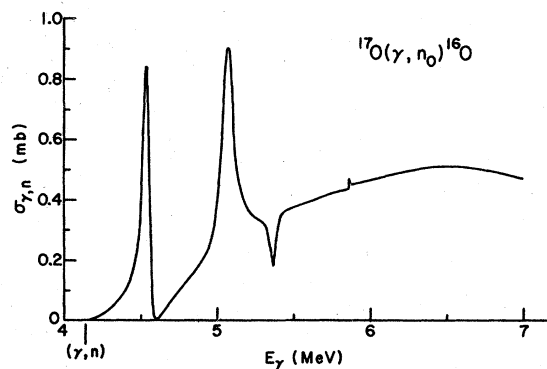


FIG. 6. Predicted total cross section for the  $^{17}\text{O}(\gamma, n_0)^{16}\text{O}$  reaction.

we note that the radiation width  $\Gamma_{\gamma_0}$  observed for the 4.55-MeV resonance is an order of magnitude less than the total radiative width reported in Ref. 9. This suggests that nonresonant direct capture to the ground state gives rise to approximately  $1.5 \mu\text{b}$  of  $\langle\sigma\rangle_{0, kT=30}$ . Therefore, it is not a valid procedure to ignore nonresonant capture in light elements where the reduced widths of resonances can be large. Even though our findings indicate that the neutron capture rate of  $^{16}\text{O}$  at  $kT=30$  keV is *at least* an order of magnitude greater than previously believed, the rate is not sufficient to inhibit the  $s$  process. However, it is possible that reaction rates for other nuclei, where the Macklin-Gibbons formula has been applied, might also be underestimated. Although further investigation of neutron capture rates clearly is indicated, it is beyond the scope of the present work.

### VIII. CONCLUSIONS

The differential cross section for the  $^{17}\text{O}(\gamma, n_0)^{16}\text{O}$  reaction was observed for the first time throughout the excitation energy range 4.3–7 MeV and at reaction angles of  $90^\circ$  and  $135^\circ$ . A self-consistent multilevel  $R$ -matrix analysis was performed of the data. The analysis included consideration of both the neutron and photon channels. All features of a general radiative capture theory were exhibited unambiguously in the  $^{17}\text{O}(\gamma, n_0)^{16}\text{O}$  spectrum. The interplay among internal, channel, and potential capture was studied in detail. The 5.38-MeV,  $\frac{3}{2}^-$  resonance was observed to be a symmetric

minimum in the cross section. This was shown to be due to a unique feature of channel capture. In addition, the 5.08-MeV  $d_{5/2} \rightarrow d_{3/2}$  spin-flip excitation was found to have an anomalously low reduced transition probability, approximately  $\frac{1}{3}$  of the single-particle estimate. The data indicates the need for a shell-model calculation which includes the  $1d_{3/2}$  orbital. The ground-state radiation width of the 4.55-MeV,  $\frac{3}{2}^-$  level was found to be approximately half the value predicted by the weak coupling model. Finally, the neutron capture rate in a stellar medium of temperature  $kT=30$  keV was estimated. This rate was found to be at least an order of magnitude larger than previously believed. This is due to a previous misapplication of the Macklin-Gibbons formula and also to the relatively large radiative direct capture component which is present in the  $^{16}\text{O}+n$  system.

We wish to thank R. D. Lawson, A. J. Elwyn, D. Kurath, J. P. Schiffer, J. E. Lynn, and F. Coester for some very informative discussions. Finally we thank G. Mavrogenes, L. Rawson, D. Ficht, B. Clift, and J. Becker for providing the reliable pico pulse electron beam from the accelerator.

### APPENDIX

In order to evaluate the integrals in Eqs. (6), (7), and (12), the angular integrations were performed explicitly. For  $E\mathcal{L}$  transitions the matrix element becomes

$$\begin{aligned} \langle \Psi_{f(J_f)} \| H^{(E\mathcal{L})} \| \begin{Bmatrix} I_i \\ O_i \end{Bmatrix} \varphi_c \rangle &= (-1)^{J_f - J - 1} \left( \frac{1}{2\pi R} \right)^{1/2} \bar{e} [(2l+1)(2J+1)(2\mathcal{L}+1)(2J_f+1)]^{1/2} \\ &\times (l\mathcal{L}00/l_f 0) W(\mathcal{L} l_f J_s; l J_f) \theta_{i_f J_f} \int_R^\infty dr r^{\mathcal{L}} \frac{W_{i_f}(k_f r)}{W_{i_f}(k_f R)} \begin{Bmatrix} I_i(kr) \\ O_i(kr) \end{Bmatrix}, \end{aligned}$$

where  $\bar{e}$  is the effective charge:  $\bar{e} = -Ze/A$  for neutrons and  $Ne/A$  for protons. For the  $M1$  transitions the matrix element is given by

$$\begin{aligned} \langle \Psi_{f(J_f)} \| H^{(M1)} \| \begin{Bmatrix} I_i \\ O_i \end{Bmatrix} \varphi_c \rangle &= \left( \frac{3}{2\pi R} \right)^{1/2} \theta_{i_f J_f} \left( \frac{e\hbar}{2M_p c} \right) (2s+1) [(2J+1)(2J_f+1)]^{1/2} W(1sJl; sJ_f) \\ &\times \left[ (2i_n+1)^{1/2} W(1i_n s i_{A-1}; i_n s) \begin{pmatrix} i_n+1 \\ i_n \end{pmatrix}^{1/2} \mu_n + (2i_{A-1}+1)^{1/2} W(1i_{A-1} s i_{A-1} s) \begin{pmatrix} i_{A-1}+1 \\ i_{A-1} \end{pmatrix}^{1/2} \mu_{A-1} \right] \\ &\times \int_R^\infty dr \frac{W_{i_f}(k_f r)}{W_{i_f}(k_f R)} \begin{Bmatrix} I_i(kr) \\ O_i(kr) \end{Bmatrix}, \end{aligned}$$

where  $i_n$  and  $i_{A-1}$  are the spins of the neutron and the daughter nucleus, respectively, and  $\mu_n$  and  $\mu_{A-1}$  are the magnetic moments in nuclear magnetons of the neutron and the daughter nucleus.

The use of the Whittaker function [Eq. (10)] for the radial part of the bound-state wave function of  $^{17}\text{O}$  represents, possibly, the most severe assumption in the present work. However, one would expect that the details of the potential-well shape would have a small effect on the radial integral in the external region. In fact, the Whittaker function is the analytic continuation of any radial wave function, in the external region, which is a bound-state solution of the Schrödinger equation with a central potential. The radial integrations implied by the above two equations were performed numerically.

- \*Work performed under the auspices of the U.S. Department of Energy.
- <sup>1</sup>G. M. Hale and D. C. Dodder, in *Proceedings of the International Conference on the Interactions of Neutrons with Nuclei*, Lowell, 1976, edited by E. Sheldon (National Technical Information Service, Springfield, Virginia, 1976), p. 1459; R. J. Holt, F. W. K. Firk, R. Nath, and H. L. Schultz, Nucl. Phys. A213, 147 (1973); J. E. Bond and F. W. K. Firk, *ibid.* A287, 317 (1977).
- <sup>2</sup>A. M. Lane and J. E. Lynn, Nucl. Phys. 17, 563 (1960); J. E. Lynn, *The Theory of Neutron Resonance Reactions* (Oxford Univ. Press, New York, 1968), p. 291.
- <sup>3</sup>M. Beer, M. A. Lone, R. E. Chrien, O. A. Wasson, M. R. Bhat, and H. R. Muether, Phys. Rev. Lett. 20, 340 (1968); M. Lubert, N. C. Francis, and R. C. Block, Nucl. Phys. A230, 83 (1974).
- <sup>4</sup>C. B. Dover and N. Van Giai, Nucl. Phys. A177, 559 (1971); J. George and R. J. Philpott, Phys. Rev. Lett. 32, 901 (1974); J. George and R. J. Philpott, Phys. Rev. C 12, 658 (1975); C. M. Vincent and H. T. Fortune, *ibid.* 2, 782 (1970).
- <sup>5</sup>T. Engeland and P. J. Ellis, Nucl. Phys. A181, 368 (1972).
- <sup>6</sup>G. E. Brown and A. M. Green, Nucl. Phys. 75, 401 (1966); A. P. Zuker, B. Buck, and J. B. McGrory, Phys. Rev. Lett. 21, 39 (1968); A. M. Bernstein, Ann. Phys. (N.Y.) 69, 19 (1972).
- <sup>7</sup>G. T. Hickey, F. W. K. Firk, R. J. Holt, and R. Nath, Nucl. Phys. A225, 470 (1974).
- <sup>8</sup>R. L. Macklin and J. H. Gibbons, Rev. Mod. Phys. 37, 166 (1965).
- <sup>9</sup>B. J. Allen and R. L. Macklin, Phys. Rev. C 3, 1737 (1971).
- <sup>10</sup>H. E. Jackson and E. N. Strait, Phys. Rev. C 4, 1314 (1971).
- <sup>11</sup>C. H. Johnson, Phys. Rev. C 7, 561 (1973).
- <sup>12</sup>R. W. Carr and J. E. Baglin, Nucl. Data Tables 10, 143 (1971).
- <sup>13</sup>A. M. Lane and R. G. Thomas, Rev. Mod. Phys. 30, 257 (1958).
- <sup>14</sup>H. E. Jackson and R. E. Toohey, Phys. Rev. Lett. 29, 379 (1972); H. E. Jackson, Phys. Rev. C 9, 1148 (1974).
- <sup>15</sup>R. Christy and I. Duck, Nucl. Phys. 24, 89 (1961).
- <sup>16</sup>T. A. Tombrello and P. D. Parker, Phys. Rev. 131, 2582 (1963).
- <sup>17</sup>C. Rolfs, Nucl. Phys. A217, 29 (1973).
- <sup>18</sup>J. J. Domingo, Nucl. Phys. 61, 39 (1965).
- <sup>19</sup>I. M. Naqib and L. L. Green, Nucl. Phys. A112, 76 (1972).
- <sup>20</sup>C. J. Oliver, P. D. Forsyth, J. L. Hutton, G. Kayle, and J. R. Mines, Nucl. Phys. A127, 567 (1969).
- <sup>21</sup>J. C. Armstrong and K. S. Quisenberry, Phys. Rev. 122, 150 (1961).
- <sup>22</sup>G. Konopka, M. Gari, and J. G. Zabolitzky, Nucl. Phys. A290, 360 (1977).
- <sup>23</sup>T. Erikson and G. E. Brown, Nucl. Phys. A277, 1 (1977); G. E. Brown, private communication.